Chaotic dynamics in yeast glycolysis under periodic substrate input flux

Mario Markus, Dietrich Kuschmitz and Benno Hess

Max-Planck-Institut für Ernährungsphysiologie, Rheinlanddamm 201, 4600 Dortmund 1, FRG

Received 9 April 1984

The numerical analysis for a glycolytic model containing the enzymes phosphofructokinase and pyruvate kinase reveals different types of entrainment, as well as chaotic response under sinusoidal substrate input. Entrainment with response periods 1, 2, 3, 5 and 7-times the input flux period and aperiodic behaviour is verified by measurements of NADH fluorescence in extracts of *Saccharomyces cerevisiae* in the theoretically predicted range. The stroboscopic transfer function obtained from the aperiodic signal admits period 3, implying chaos according to the Li–Yorke theorem.

Oscillation *Chaos* *Entrainment* *Glycolysis* *Yeast*

1. INTRODUCTION

A previous experimental and theoretical study of oscillatory glycolysis in yeast extracts under a periodic source of glucose revealed periodic responses with periods 1, 2 and 3-times the input flux period [1]. Recently, a more detailed theoretical investigation was reported [2,3] yielding a rich variety of time patterns, including additional modes of entrainment and chaotic response. A prediction of such effects in an experimentally feasible range and its experimental verification are reported here.

Abbreviations: PFK, phosphofructokinase (EC 2.7.1.11); PK, pyruvate kinase (EC 2.7.1.40); FBP, fructose 1,6-bisphosphate; F6P, fructose 6-phosphate; PEP, phospho*enol*pyruvate; $[K_{tot}]$ and $[Mg_{tot}]$, total concentrations (bound plus unbound) of potassium and magnesium; F, NADH fluorescence in arbitrary units; ω_e, T_e, frequency and period of the externally (e) applied flux; ω, T, frequency and period of the system response; ω_0, T_0, frequency and period of the system at constant input flux, i.e., without periodic excitation

2. MATERIALS AND METHODS

Cell-free extracts were prepared from commercial baker's yeast (*S. cerevisiae*) as in [4]. Protein contents, as determined with the Biuret method, ranged from 41 to 55 mg/ml. For experimentation, 1 ml of extract was diluted with 1 ml of 0.1 M K-phosphate (pH 6.4) and NADH was measured fluorimetrically [1] at room temperature. Continuous and periodic injection of 0.3 M glucose into the sample cuvette was performed with a Precidor HT-pump (Infors, Basel) modified to allow external electric speed control with a function generator (Wavetec 145). The input flux rate of glucose was adjusted in each yeast extract preparation to match a standard period of oscillation without external periodic excitation ($T_0 \approx 12$ min), as given in fig.1a.

3. MODEL

The model is based on the following assumptions. Only the enzymes PFK and PK are considered. F6P, which is consumed by PFK, is supplied as input. To simplify the calculations, the intermediate part of glycolysis, accounting for the con-

Published by Elsevier Science Publishers B.V.
00145793/84/$3.00

sumption of FBP and production of PEP is neglected. Instead, FBP accumulates starting from [FBP] = 5 mM. This FBP concentration is a saturating value with respect to the activation of PK. PEP, which is consumed by PK, is supplied as input. ATP (or ADP), which is consumed by PFK (or PK) is recycled by PK (or PFK). This system is described by the following differential equations [2,3]:

$$\frac{d[F6P]}{dt} = \frac{d[PEP]}{dt} + \frac{d[ATP]}{dt} = \bar{V}_{in} + A\sin\omega_e t - V_{PFK} \quad (1)$$

$$\frac{d[ADP]}{dt} = -\frac{d[ATP]}{dt} = V_{PFK} - V_{PK} \quad (2)$$

where $\bar{V}_{in}$ is the mean input flux; A and ω_e are the amplitude and the frequency of the periodic input flux; V_{PK} and V_{PFK} are the enzymic rates. For V_{PK}, we use the rate law in [5] depending on [PEP], [ADP], [ATP], [Mg^{2+}] and [K^+]. Complex formation of magnesium and potassium with the ligands is considered as in [6]. For V_{PFK}, we use the rate law in [7] depending on [F6P], [ATP], [ADP] and [PEP], under the additional assumption of random substrate binding of substrates with dissociation constants independent of the binding order. The accumulating products pyruvate and FBP, where [FBP] > 5 mM, do not affect the kinetics of the enzymes over a wide range of concentrations.

We normalized the fluxes dividing them by $V_{max(PK)}$, and the time (or frequency) dividing it by $K_{PEP}/V_{max(PK)}$ (or $V_{max(PK)}/K_{PEP}$), where K_{PEP} = 0.31 mM is a dissociation constant given in [5]. Using this normalization, it can be shown that the dynamics of the system depend on the following parameters: $\nu = \bar{V}_{in}/V_{max(PK)}$, $\alpha = A/V_{max(PK)}$, $\epsilon = V_{max(PFK)}/V_{max(PK)}$, $\tilde{\omega}_e = \omega_e K_{PEP}/V_{max(PK)}$, C = [PEP] + [ATP] − [F6P], [ADN] = [ADP] + [ATP], [Mg_{tot}] and [K_{tot}]. For calculations, we set: $\nu = \alpha$ = 0.12, ϵ = 0.34, [ADN] = 2.55 mM, C = 5.75 mM, [Mg_{tot}] = 5 mM, [K_{tot}] = 200 mM. We integrate the differential equations using the program DCO1AD from [8].

4. RESULTS

In the absence of periodic excitation, the calculations yielded oscillations having a normalized frequency $\tilde{\omega}_0 = \omega_0 K_{PEP}/V_{max(PK)}$ = 0.13, the normalized input flux being $\nu = \bar{V}_{in}/V_{max(PK)}$ = 0.12. Assuming $V_{max(PK)}$ = 1.4 mM/min, we obtain $\bar{V}_{in}$ = 10 mM/h and a period T_0 = 11 min. This matches well with the experimental result shown in fig.1a, where $\bar{V}_{in}$ = 12 mM/h and T_0 = 12 min.

Fig.1b–d shows the results obtained at different frequencies of the periodic excitation. Fig.1b displays chaotic behaviour. Fig.1c,d shows oscillations having periods 5- and 3-times the input period, respectively. The last type of response has been reported [1]. The mean input fluxes, which were adjusted as described in section 2, are $\bar{V}_{in}$ = 24, 6 and 12 mM/h in fig.1b,c,d, respectively. For oscillating input we set $\bar{V}_{in} \perp A$

The oscillations shown in fig.1 are displayed after being corrected for a systematic linear drift of NADH fluorescence. The relative drift, defined by $\Delta F/(F_{max} - F_{min})$, where F is the measured signal and ΔF its change due to the drift, amounted to 0.05 per oscillation period for fig.1a and 0, 0.027 and 0.011 per input flux period in fig.1b,c,d, respectively.

Fig.2a,b shows the theoretical and experimental results, respectively, over a wide range of input flux

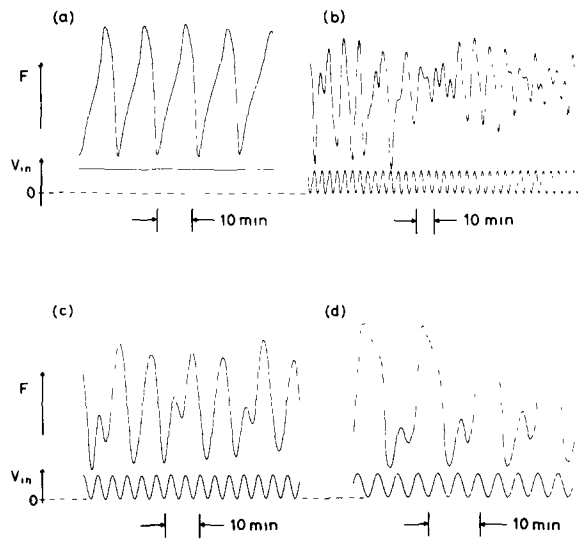

Fig.1. Measured NADH fluorescence (upper) for different time dependences of the glucose input flux (lower). All ordinate units are arbitrary. (a) Oscillations at constant input flux; (b) ω_e/ω_0 = 2.76, yielding chaos; (c) ω_e/ω_0 = 2.82, yielding period T/T_e = 5; (d) ω_e/ω_0 = 3.12, yielding period T/T_e = 3.

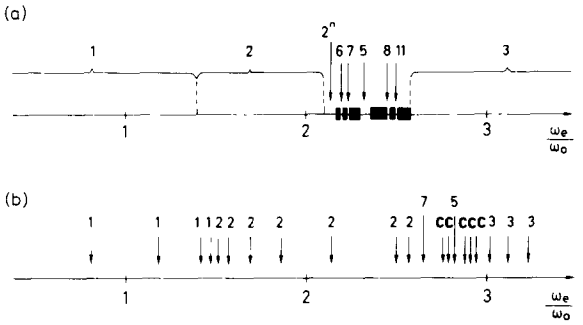

Fig.2. Theoretical (a) and experimental (b) dependence of the system response on the input flux frequency ω_e divided by the system frequency ω_0 at constant input flux. The numbers above the lines indicate the response period relative to the input flux period. 2^n indicates a period doubling sequence from left to right. Chaos is indicated by dark blocks in (a) and by C in (b).

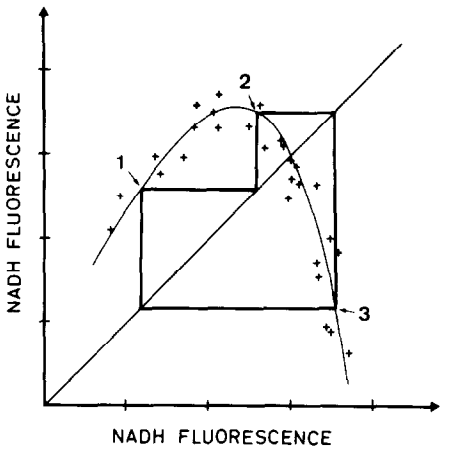

Fig.3. Stroboscopic transfer function corresponding to the chaotic response shown in fig.1b. (+) Measured signal (arbitrary units) at an input flux maximum *vs* the signal at one maximum before. The closed solid line shows that the transfer function admits period 3 (see numbers).

frequencies. The numbers above the lines are the quotients between the response period T and input flux period T_e. The numerical results displayed in fig.2a reveal a bifurcation from $T/T_e = 1$ to $T/T_e = 2$ at $\omega_e/\omega_0 = 1.4$. At $\omega_e/\omega_0 = 2.1$, a new period doubling is obtained and – on increasing ω_e/ω_0 – a period doubling cascade ($T/T_e = 2^n$) follows ending up in chaos, as described in [9]. The chaotic region at $2.17 \leq \omega_e/\omega_0 \leq 2.58$ contains windows with periods $T/T_e = 6$, 7, 5, 8 and 11. Chaos is approached from these windows on increasing frequency by period doubling sequences (not shown). Period $T/T_e = 3$ appears for $\omega_e/\omega_0 > 2.58$.

In the corresponding experiments (fig.2b), we observe the bifurcation from $T/T_e = 1$ to $T/T_e = 2$ at $\omega_e/\omega_0 \cong 1.5$, which is close to the theoretically predicted value of 1.4. The chaotic region occurs at somewhat larger frequencies than those predicted. Two of the predicted windows are observed, namely $T/T_e = 7$ and 5. We were not able to detect chaos between $T/T_e = 2$ and 7, possibly because experimentation did not allow us to hit the corresponding chaotic region.

To obtain evidence that a given measured oscillation is chaotic, we determined its stroboscopic transfer function, as shown in fig.3 for the oscillation given in fig.1b. In this representation, we plotted the measured signal at a maximum of the input flux *vs* the signal at one maximum before. We thus obtained a single-valued transfer function. As shown, this function permits us to construct a sequence of points with a period equal to 3 transitions, as given by the numbers 1, 2, 3 in the figure. Authors in [10] have shown that the existence of such a sequence of period 3 allows for chaotic behaviour of the system. As a further diagnostic procedure, we determined power spectra [11] and stroboscopic plots in the phase plane determined by F and dF/dt [12]. As for power spectra, chaotic oscillations showed larger broad-band noise than periodic oscillations, and in some cases investigated here yielded almost continuous spectra. In addition, the stroboscopic plots of the chaotic regimes in the $F - dF/dt$ plane revealed stretching, folding and pressing of the attracting region upon variation of the phase at which the solution is plotted, similar to the chaotic membrane potential response of *Onchidium* giant neuron under periodic electric perturbation [12].

5. DISCUSSION

Upon periodic perturbation of a non-linear oscillator, a rich variety of time patterns, including chaotic behaviour, is predicted theoretically. Our results show that a biochemical system under periodic substrate influx displays chaos, as well as unusual periodicities (periods $T/T_e = 5$ and 7). The experiments are in satisfactory agreement with the

model prediction, despite the fact that a simplified model was used for calculation of the dynamics of glycolysis, supporting the PFK oscillator theory. The finding of only two of the predicted periodic windows in the chaotic region may be due to their narrowness, which hinders their experimental detection.

The time patterns of a non-linear system resulting from periodic perturbation, as investigated here, may be relevant in physiological processes, as occur in intra- and/or intercellular dynamic coupling, for example in neural systems. Similar results to those here have been obtained upon periodic electric perturbation of *Onchidium* giant neurons [12] and *Nitella* [13], however theoretical predictions on the basis of rate laws have not been made. It should further be mentioned that autonomous chaos (in the absence of external perturbation) has been demonstrated in biochemical systems. In glycolysis, autonomous chaos has been described theoretically [14]. In the peroxidase–oxidase reaction autonomous chaos has been investigated both theoretically and experimentally [15].

Recently, we found that a much higher degree of randomness in chaotic responses may be obtained if periodic amplitude and frequency modulation of the sinusoidal input flux is included in the theoretical calculations. Experimental analysis of these novel dynamic states is currently under investigation.

ACKNOWLEDGEMENTS

We thank Mr U. Heidecke and Mrs I. Schlieker for their help in the laboratory, Mr H. Schlüter for assistance in the electronic set-up, and Mr H. Becher for computing assistance.

REFERENCES

[1] Boiteux, A., Goldbeter, A. and Hess, B. (1975) Proc. Natl. Acad. Sci. USA 72, 3829–3833.
[2] Hess, B. and Markus, M. (1984) in: Synergetics – From Microscopic to Macroscopic Order (Frehland, E. ed.) pp. 6–16, Springer-Verlag, Berlin.
[3] Markus, M. and Hess, B. (1984) Proc. Natl. Acad. Sci. USA 81, in press.
[4] Hess, B. and Boiteux, A. (1968) Hoppe-Seyler's Z. Physiol. Chem. 349, 1567–1574.
[5] Boiteux, A., Markus, M., Plesser, T., Hess, B. and Malcovati, M. (1983) Biochem. J. 211, 631–640.
[6] Markus, M., Plesser, T., Boiteux, A., Hess, B. and Malcovati, M. (1980) Biochem. J. 189, 421–433.
[7] Blangy, D., Buc, H. and Monod, J. (1968) J. Mol. Biol. 31, 13–35.
[8] Harwell Subroutine Library (1973) A Catalogue of Subroutines, Theoretical Physics Division, A.E.R.E., Harwell.
[9] Feigenbaum, M. (1978) J. Stat. Phys. 19, 25–52; (1979) J. Stat. Phys. 21, 669–706.
[10] Li, T.Y. and Yorke, J.A. (1975) Am. Math. Mon. 82, 985–992.
[11] Kubíček, M. and Marek, M. (1983) Computational Methods in Bifurcation Theory and Dissipative Structures, pp. 109–111, Springer Verlag, New York.
[12] Hayashi, H., Ishisuka, S., Ohta, M. and Hirakawa, K. (1982) Phys. Lett. 88A, 435–438.
[13] Hayashi, H., Nakao, M. and Hirakawa, K. (1982) Phys. Lett. 88A, 265–266.
[14] Decroly, O. and Goldbeter, A. (1982) Proc. Natl. Acad. Sci. USA 79, 6917–6921.
[15] Olsen, L.F. (1984) in: Stochastic Phenomena and Chaotic Behaviour of Complex Systems (Schuster, P. ed.) pp. 116–123, Springer Verlag, Berlin.